On stability of time marching in numerical solutions of rayleigh-plesset equation for ultrasonic cavitation

Wah Yen Tey[1,2,*], Habib Alehossein[3], Zonyi Qin[4], Kiat Moon Lee[5], Hooi Siang Kang[6] and Kee Quen Lee[2]

1 Department of Mechanical Engineering, Faculty of Engineering, UCSI University, Kuala Lumpur, Malaysia
2 Malaysia-Japan International Institute of Technology, Universiti Teknologi Malaysia, Kuala Lumpur, Malaysia
3 School of Civil Engineering and Surveying, University of Southern Queensland, Australia
4 Mineral Resources, Commonwealth Scientific and Industrial Research Organisation, Australia
5 Department of Chemical and Petroleum Engineering, Faculty of Engineering, UCSI University, Kuala Lumpur, Malaysia
6 School of Mechanical Engineering, Faculty of Engineering, Universiti Teknologi Malaysia, Johor Bahru, Malaysia
7 Marine Technology Centre, Institute for Vehicle System and Engineering, Universiti Teknologi Malaysia, Johor Bahru, Malaysia

* E-mail: Wahyen.Tey@gmail.com or teywy@ucsiuniversity.edu.my

Abstract. Ultrasonic irradiation approach has become one of the most popular methods applied in chemical processing including lignocellulosic biomass pretreatment and industrial cleansing. The phenomenon of ultrasonic cavitation can be indeed delineated via the Rayleigh-Plesset equation (RPE), which governs the transient radius of the bubble. Nonetheless, the time marching in the numerical solutions for RPE is highly unstable, which cannot be assured using von Neumann analysis. High sensitivity of RPE to time step may lead to extremely long computational time. The lack of numerical investigation into the time stepping issue of RPE has hindered in-depth simulation of ultrasonic cavitation. Therefore, the purpose of this paper is to investigate the stability criterion of time stepping for RPE in different time progression schemes, namely Euler explicit, 2nd order Taylor's method, 4th order Runge-Kutta, Runge-Kutta Fehlberg and Cash-Karp Runge-Kutta method. A simple modified adaptive time step method and α independence study has been introduced in this paper for fast, stable and accurate computation of RPE. Compared with the traditional constant time marching method, the new model is able to improve the computational cost significantly without affecting the time marching stability and resolution of the results. Among the investigated method, Runge-Kutta family solvers have higher computational accuracy, with the cost of higher critical α value. The model is also applied to compute the pressure and temperature hike during bubble collapse due to different sonication power. The simulation results show that the ultrasonic irradiation with higher sonication power could produce a higher energy to break the lignocellulose wall.

1. Introduction

Ultrasonic irradiation has been widely applied in the field of green energy and environment such as disruption of lignocellulose in lipid extraction [1,2] and degradation of sludge [3,4]. This can be due to its high efficiency and environmental benign treatment properties [1,2,5,6]. Experimental optimisations of ultrasonic pretreatment have been reported in many works [7–12]. Indeed, the core of ultrasonic pretreatment lies the cavitation process [4,13,14], while the physics of cavitation is governed by Rayleigh-Plesset Equation (RPE). RPE was proposed and developed by Rayleigh [15] and Plesset [16,17] to mathematically represent the growth of bubble radius arisen by the acoustic cavitation.

The formation of RPE follows several important assumptions [18,19]: (a) both the geometry and geometrical deformation of bubble exists in spherical shape; (b) the growing or collapse speed of the bubble is less than the speed of sound (i.e. the size of the bubble is less than the acoustic wavelength); (c) the fluid is Newtonian and homogenous; and (d) body forces such as gravitational and centrifugal force are ignored. If there is discrepancy between the actual physical condition and assumed condition will negate RPE, further specific mathematical treatment is required [20].

In RPE, the bubble radius is a function of the time. Although RPE resembles hyperbolic equation, it does not have any boundary value and therefore can be regarded as initial value problem or ordinary differential equation. In other words, the von Neumann analysis [21] which correlates the size of domain with the time step, is no longer applicable for RPE. The mathematical singularity at infinitely small value of radius will lead to highly fluctuating numerical results [22]. Adaptive time-step technique in solving RPE was firstly put forward by Alehossien and Qin [22] using Euler and Runge-Kutta (RK) method, and their model is able to deal with the sharp rate of change of radius during bubble collapse and rebound. Adaptive time-stepping RK is then applied by Tian et al. [23], Chakma and Moholkar [24] and Sajjadi et al. [13] in their works to study the effects of different parameters to ultrasonic pretreatment efficiency. Merouani and co-workers [25–27] computed the bubble radius and other related parameters via constant time-step RK method yet without further specifying the value of time step. The similar limitation goes to the work of Tey et al. [28]. These results on history of bubble growth is different with the works of [13,22–24]. It is also noteworthy that the radius of bubble drops smoothly according to the work of Fourest et al. [18], Narendranath [29] and Ghahramani et al. [30], which is in contradictory with the "bouncing" radius pattern as obtained by [22–25,27].

The result of the growth and collapse of bubble is indeed inconclusive. Moreover, there is a lack of discussion in stability criterion of the time progression model. Therefore, the focus of the work is to investigate the time-marching stability of discretised RPE in different time-stepping schemes. In order to stabilise the time marching of discretised RPE, a modified adaptive time stepping method is introduced in this paper. The method is easy to implement, and able to significantly save computational cost as compared to previous available solvers. Time progression models being tested under the new method includes Euler explicit, 2nd Taylor's method, 4th order Runge-Kutta, Runge-Kutta Fehlberg and Cash-Karp Runge-Kutta method will be applied. Instantaneous bubble radius, bubble growth/collapse speed, pressure hike and temperature hike due to different ultrasonic power are computed and compared.

2. Rayleigh-Plesset Equation

Referring to the schematics of single air bubble which is surrounded by the fluid volume, its cylindrical coordinate momentum equation [31] in one-dimensional *r*-component vector can be expressed as:

$$\frac{\partial u_r}{\partial t} + u_r \frac{\partial u_r}{\partial r} = -\frac{1}{\rho}\left(\frac{\partial P}{\partial r} + \frac{\partial \tau_w}{\partial r}\right) \tag{1}$$

where u_r, ρ and τ_w is the speed of growth of bubble, density of the gas inside the bubble and the wall shear stress on the surface of the bubble.

For irrotational flow u_r can be related with velocity potential ϕ as in Equation (2). Equation (2) is then combined with Equation (1) to form Equation (3).

$$u_r = \frac{\partial \phi}{\partial r} \tag{2}$$

$$\frac{\partial}{\partial t}\left(\frac{\partial \phi}{\partial r}\right) + \left(\frac{\partial \phi}{\partial r}\right)\frac{\partial}{\partial r}\left(\frac{\partial \phi}{\partial r}\right) = -\frac{1}{\rho}\left(\frac{\partial P}{\partial r}\right) \tag{3}$$

To ensure the conservation of the mass, Continuity principle as in Equation (4) can be applied to form an operator which relates the velocity potential with the radius of the bubble *R*. The equation which links velocity potential and the bubble radius can be formulated as shown in Equation (6), by combining Equation (5) and Equation (2).

$$\frac{\partial}{\partial r}\int_{CV}\rho dV+\int_{CS}\rho\left(\mathbf{v}.\vec{\mathbf{n}}\right)dA=0 \tag{4}$$

$$u_r\left(4\pi r^2\right)=u_R\left(4\pi R^2\right)\rightarrow u_r=u_R\frac{R^2}{r^2} \tag{5}$$

$$\frac{\partial r}{\partial t}=\frac{\partial R}{\partial t}\frac{R^2}{r^2} \tag{6}$$

Integration on Equation (6) with respect to component *r* will yield Equation (7). When *r* = *R*, Equation (7) will become Equation (8).

$$\phi(r)=-\frac{\partial R}{\partial t}\frac{R^2}{r} \tag{7}$$

$$\phi(R)=-\frac{\partial R}{\partial t}\frac{R^2}{R}=-R\frac{\partial R}{\partial t} \tag{8}$$

The derivative of Equation (3) is then changed from *r* to *R* before an integration is executed. The integration by substitution can be applied to integrate the second term of the left-hand side of Eq. (3), with its answer as shown in Equation (9). Equation (3) will then evolve into Equation (10). With this mathematical treatment Equation (8) will be applicable for incorporation into Equation (10) to form Equation (11).

$$\int\left(\frac{\partial\phi}{\partial r}\right)\frac{\partial}{\partial r}\left(\frac{\partial\phi}{\partial r}\right)dr=\int qdq\Big|_{q=\frac{\partial\phi}{\partial r},\frac{\partial q}{\partial r}=\frac{\partial}{\partial r}\left(\frac{\partial\phi}{\partial r}\right),\partial r=\partial q\div\frac{\partial}{\partial r}\left(\frac{\partial\phi}{\partial r}\right)}=\frac{q^2}{2}=\frac{1}{2}\left(\frac{\partial\phi}{\partial r}\right)^2 \tag{9}$$

$$\frac{\partial\phi}{\partial t}+\frac{1}{2}\left(\frac{\partial\phi}{\partial r}\right)^2=-\frac{\Delta P}{\rho} \tag{10}$$

$$\frac{3}{2}\left(\frac{\partial R}{\partial t}\right)^2+R\frac{\partial^2 R}{\partial t^2}=\frac{\Delta P}{\rho} \tag{11}$$

With inclusion of surface tension term and viscosity term as in Equation (12) and (13) respectively, Equation (11) can be modified to form Equation (14) as Rayleigh-Plesset equation.

$$2\pi R\sigma_s=dP\pi R^2\rightarrow dP=\frac{2\sigma_s}{R}\rightarrow P_i=P_e+\frac{2\sigma_s}{R} \tag{12}$$

$$\tau_w=\tau_{rr}=2\mu\frac{\partial u_r}{\partial r}=2\mu\frac{\partial}{\partial r}\left(\frac{\partial r}{\partial t}\right)=2\mu\frac{\partial}{\partial r}\left(\frac{\partial R}{\partial t}\frac{R^2}{r^2}\right)=-4\mu\frac{R^2}{r^3}\frac{\partial R}{\partial t}=-\frac{4\mu}{R}\frac{\partial R}{\partial t} \tag{13}$$

$$\frac{3}{2}\left(\frac{\partial R}{\partial t}\right)^2+R\frac{\partial^2 R}{\partial t^2}=\frac{1}{\rho}\left(P_v+P_g\left(\frac{R_0}{R}\right)^{3\eta}-P_\infty-\frac{2\sigma_s}{R}-\frac{4\mu}{R}\frac{\partial R}{\partial t}\right) \tag{14}$$

where η, σ_s, μ, R_0, P_i and P_e is the ratio between specific heat capacities (C_P/C_V), surface tension, dynamic viscosity, initial bubble radius, internal bubble pressure and external bubble pressure respectively. The internal pressure is composed of the vapor pressure P_v and gas pressure P_g. P_∞ represents the pressure fluctuation due to ultrasonic irradiation.

3. Stable RPE Modelling via Modified Adaptive Time-Stepping Method

RPE as in Equation (14) can be re-written as in Equation (15), which is indeed an ordinary differential equation.

$$\frac{\partial v}{\partial t}=\frac{1}{R}\left[\frac{1}{\rho}\left(P_v+P_g\left(\frac{R_0}{R}\right)^{3\eta}-P_\infty-\frac{2\sigma_s}{R}-\frac{4\mu v}{R}\right)-\frac{3}{2}v^2\right]\Bigg|v=\frac{\partial R}{\partial t} \tag{15}$$

The applied value for surface tension, dynamic viscosity, initial bubble, vapor pressure and gas pressure is 7×10^{-2} N/m, 0.001015 Pa.s, 2×10^{-6} m, 10000 Pa and 400 Pa respectively. The initial growth

speed v is 0 m/s while η is assumed as 1.4. The pressure fluctuation P_∞ is indeed resulted by ultrasonic irradiation, correlated with the power W of the ultrasonic transducer via Equation (16) and (17):

$$P_\infty = 101325 + P_{amp}\sin(2\pi ft) \tag{16}$$

$$I = \frac{P^2}{\rho c^2} \rightarrow \frac{W}{A} = \frac{P^2}{\rho c^2} \rightarrow P_{amp} = \sqrt{\frac{W\rho c^2}{A}} \tag{17}$$

where W, f, ρ, c and A represents ultrasonic power, fluid's density, speed of sound in the fluid and the area of ultrasonic emission respectively. Since the speed of sound in the fluid domain is assumed to be as 1450 m/s, and by setting A = 0.1 m^2 and W = 100 W, therefore P_{amp} = 1450000 Pa. The simplest solution to Equation (15) is through Euler's explicit and 2nd order Taylor's method, which can be described as in Equation (18) and (19) respectively [32]:

$$v(t_{i+1}) = v(t_i) + \Delta t\left[f(x,t)\right] \tag{18}$$

$$v(t_{i+1}) = v(t_i) + \Delta t\left[f(x,t)\right] + \Delta t^2\left[f'(x,t)\right] \tag{19}$$

where $f = \partial v/\partial t$ while $f' = \partial^2 v/\partial t^2$. For a higher order estimation, 4th order Runge-Kutta (RK4), Runge-Kutta Fehlberg (RKF) and Cash-Karp Runge-Kutta (CKRK) can be applied, which can be expressed as in Equations (20) – (22) respectively [33]:

$$v(t_{i+1}) = v(t_i) + \frac{\Delta t}{6}\left(k_{11} + 2k_{12} + 2k_{13} + k_{14}\right) \tag{20}$$

$$v(t_{i+1}) = v(t_i) + \Delta t\left(\frac{37}{378}k_{21} + \frac{250}{621}k_{22} + \frac{125}{594}k_{23} + \frac{512}{1771}k_{24}\right) \tag{21}$$

$$v(t_{i+1}) = v(t_i) + \Delta t\left(\frac{2825}{27648}k_{21} + \frac{18575}{48384}k_{23} + \frac{13525}{55296}k_{24} + \frac{277}{14336}k_{25} + \frac{1}{4}k_{26}\right) \tag{22}$$

in which all the formulas of coefficients k can be illustrated as in Table 1.

Indeed, the time step in RPE is critical in determining the simulation performance. In most of the studies [8,13,23,24,26,30,34], the time independence study is needed if constant time-step method is applied, otherwise adaptive time-stepping method as outlined by Alehossien and Qin [22] is required. In order to handle the time-step-sensitive RPE, we introduce a modified adaptive time stepping method, which is simpler without adversely affecting the results' accuracy. The adaptive time step can be simply defined as:

$$\Delta t(t_i) = \left[R(t_i)\right]^\alpha \tag{23}$$

where α is time index. α is a real number, which can be optimised for a stable and accurate simulation. Therefore, in this paper α independence study is introduced to replace the time independence study. Upon computation on the bubble radius, the pressure and temperature of the collapsing bubble [34] can be determined using Equation (24) and (25) respectively,

$$P_{collapse} = \left[P_v + P_{g0}\left(\frac{R(t=0)}{R_{max}}\right)^3\right]\left(\frac{R_{max}}{R_{min}}\right)^{3\eta} \tag{24}$$

$$T_{collapse} = T_\infty\left(\frac{R_{max}}{R_{min}}\right)^{3(\eta-1)} \tag{25}$$

where T_∞ is the ambient liquid temperature.

4. Results and Discussion

A sample of α independence study is conducted based on Euler explicit method as described in Equation (18). The growth and radius of bubble with respect to time is illustrated in Figure 1. The applied frequency of ultrasonic irradiation is 20 kHz while the total time simulated is 2×10^{-4} s. It can be clearly shown that the higher the value of α, the better the accuracy and resolution of the solution. Moreover, a higher value of α enables the better control on the expansion and bouncing of the bubble radius, without incurring the erroneous time delay which is apparent at low α. Upon α = 1.75, the solution can be considered converged.

Table 1. Formulas of coefficients *k* of Runge-Kutta family solvers as in Equations (20) – (22).

k	Formula	k	Formula
k_{11}	$f\left(t_i, v^n\right)$	k_{21}	$f\left(t_i, v^n\right)$
k_{12}	$f\left(t_i+\frac{\Delta t}{2}, v^n+\frac{k_{11}}{2}\right)$	k_{22}	$f\left(t_i+\frac{\Delta t}{5}, v^n+\frac{k_{21}}{5}\right)$
k_{13}	$f\left(t_i+\frac{\Delta t}{2}, v^n+\frac{k_{12}}{2}\right)$	k_{23}	$f\left(t_i+\frac{3}{10}\Delta t, v^n+\frac{3k_{21}+9k_{22}}{40}\right)$
k_{14}	$f\left(t_i+\Delta t, v^n+k_{13}\right)$	k_{24}	$f\left(t_i+\frac{3}{5}\Delta t, v^n+\frac{3k_{21}-9k_{22}+12k_{23}}{10}\right)$
		k_{25}	$f\left(t_i+\Delta t, v^n+\frac{-11k_{21}+135k_{22}-140k_{23}+70k_{24}}{54}\right)$
		k_{26}	$f\left(t_i+\frac{7}{8}\Delta t, v^n+\frac{1631k_{21}+18900k_{22}+2296k_{23}+22137.5k_{24}+3415.5k_{25}}{55296}\right)$

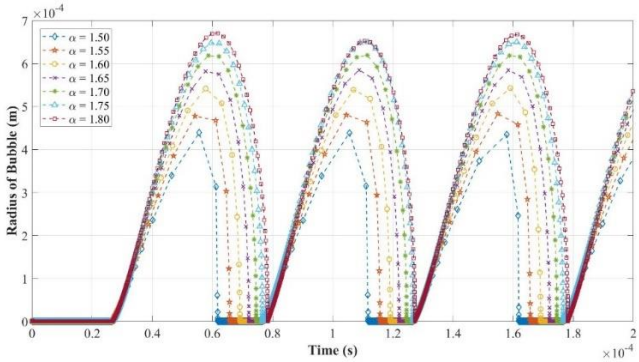

Figure 1. α independence study for RPE solution using Euler explicit method.

Indeed, high value of α implies a smaller time step for every progression. The entailing cost of higher accuracy and resolution will be the number of iterations needed, as evinced in Tables 2. The number of iterations due to α is almost similar across all types of ODE solution. We found that there is always a critical value of α in which when the applied value of α is less than critical α value, the solution will be facing singularity issue and the results will be fallacious. 2nd order Taylor's method has the lowest critical α value (1.45) while CKRK needs the largest critical α value (1.55) to enable stable computation. Within the similar α (taking 1.75 as the example), RK4, RKF and CKRK would give relatively better results compared with others, as shown in Figure 2.

The newly proposed time-adaptive method could greatly reduce the computational cost because the time step has been tuned directly with the radius using an index. The reduction of computational cost can be calculated by comparing the number of iterations required when modified adaptive time stepping method is used with the number of iterations needed if the smallest time step is applied consistently throughout every iteration. The cost ratio β between these numbers of iterations can be defined as in Equation (26). The smaller the value of β, the larger the reduced computational cost.

$$\beta = \frac{\text{No. of iteration using modified adaptive time stepping method}}{\text{No. of iteration using constant time stepping method}} \tag{26}$$

The minimum time step required for is 4.8789×10^{-18} s, which implies that the number of iterations required for constant time stepping method is 4.1×10^{13}. Such great amount of iterations would take the computer a very long time to reach a solution within a prescribed time and an extremely large memory to store the data. This is impeding an effective computation for a larger scale simulation. The cost ratio using different ODE solutions at respective α has been computed as in Table 3. In general, despite better accuracy of Runge-Kutta family solvers, they are computationally more expensive compared with Euler Explicit and 2nd order Taylor's method.

Table 2. Number of iterations needed due to α using various ODE solutions.

α	Number of iterations				
	Euler Explicit	2nd Order Taylor	RK4	RKF	CKRK
1.45	Singularity	252736	Singularity	Singularity	Singularity
1.50	450005	451316	Singularity	Singularity	Singularity
1.55	768436	768235	698749	700782	Singularity
1.60	1295965	1295837	1202724	1209013	1195939
1.65	2193757	2193647	2067388	2083431	2050566
1.70	3771650	3771467	3457126	3463737	3455329
1.75	7334816	7334814	7331581	7332822	7331477
1.80	15572244	15572242	15568449	15569983	15568393

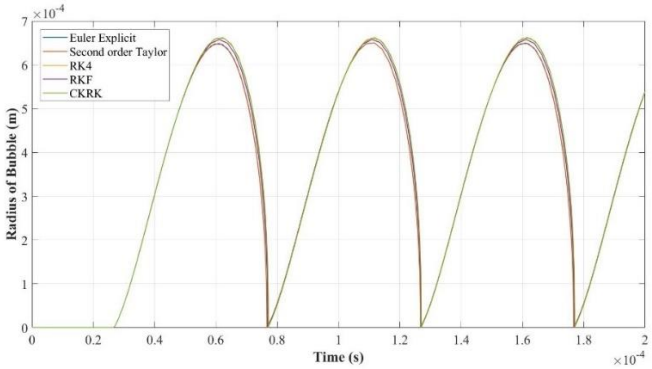

Figure 2. RPE solution due to different ODE methods at α = 1.75.

Table 3. Cost ratio β using modified adaptive time-stepping method and constant time-stepping method β due to α using various ODE solutions.

α	β (10^{-8})				
	Euler Explicit	2nd Order Taylor	RK4	RKF	CKRK
1.45	NA	0.6318	NA	NA	NA
1.50	1.1250	1.1283	NA	NA	NA
1.55	1.9211	1.9206	1.7469	1.7520	NA
1.60	3.2399	3.2396	3.0068	3.0225	2.9898
1.65	5.4844	5.4841	5.1685	5.2086	5.1264
1.70	9.4291	9.4287	8.6428	8.6593	8.6383
1.75	18.3370	18.3370	18.3290	18.3321	18.3287
1.80	38.9306	38.9306	38.9211	38.9250	38.9210
Average	**11.2096**	**9.8876**	**12.6358**	**12.6499**	**14.8009**

The model is then extended to compute the RPE solutions due to different sonication power (40W, 60W, 80W and 100W), based on CKRK at α = 1.80. The results are illustrated in Figure 3. At time of about 0.77×10^{-4} s, 1.27×10^{-4} s and 1.77×10^{-4} s, abrupt fall and rise of the bubble radius can be observed, which contributes to the very high speed of bubble growth and collapse. Indeed, the bubble implosion occurs at these moments (*hotspots*), releasing a shockwave which dissipate great energy to break the lignocellulosic wall of biomass compound [1,14]. The temperature and pressure hike at these hotspots can be calculated using Equation (24) and (25), and the results are tabulated in Figure 4. The ambient temperature T_∞ is assumed as 300K. Basically, ultrasonic irradiation with higher sonication power will release higher energy to the surrounding and therefore improve the efficiency of pretreatment [35], provided that there is no formation of dense cloud of cavitation bubbles [36].

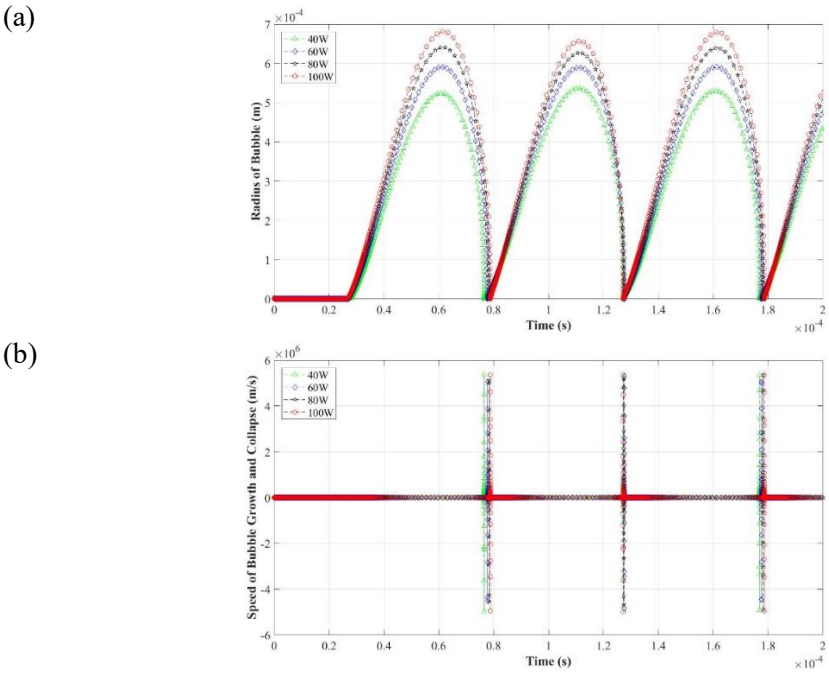

Figure 3. RPE solution of (a) radius of bubble and (b) speed of bubble growth/collapse due to various sonication power using CKRK at $\alpha = 1.80$.

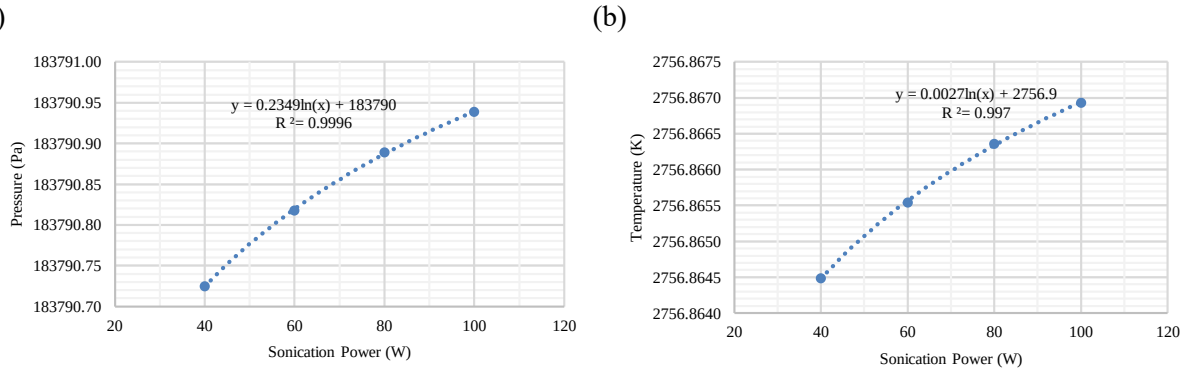

Figure 4. (a) Pressure emission and (b) temperature hike during the collapse of microbubbles due to various sonication power.

5. Conclusion

A simple modified adaptive time stepping method has been introduced in this paper for an efficient computation of time-step sensitive RPE. The model is able to handle the dramatic change of bubble radius in the hotspot while accelerating the computation speed during the steady growth of bubble. Amongst the investigated methods, Runge-Kutta family solvers are computationally more expensive (average β of 13.3622) due to its higher critical α value (1.5 – 1.55), yet with a better result accuracy and resolution. Using the modified adaptive time stepping method, the pressure and temperature hike is increased with sonication power. The proposed method is therefore enabling a more detailed investigation into the effect of various factors of ultrasonic irradiation for optimisation of biomass pretreatment.

Acknowledgments

The research is financially supported by Centre of Excellence for Research, Value Innovation and Entrepreneurship (CERVIE), UCSI University, Kuala Lumpur, Malaysia.

References

[1] Karimi M, Jenkins B and Stroeve P 2014 Ultrasound irradiation in the production of ethanol from biomass *Renew. Sustain. Energy Rev.* **40** 400–21
[2] Zou S, Wang X, Chen Y, Wan H and Feng Y 2016 Enhancement of biogas production in anaerobic co-digestion by ultrasonic pretreatment *Energy Convers. Manag.* **112** 226–35
[3] Onyeche T I, Schläfer O, Bormann H, Schröder C and Sievers M 2002 Ultrasonic cell disruption of stabilised sludge with subsequent anaerobic digestion *Ultrasonics* **40** 31–5
[4] Pilli S, Yan S, Bhunia P, Tyagi R D, Surampalli R Y and LeBlanc R J 2010 Ultrasonic pretreatment of sludge: A review *Ultrason. Sonochem.* **18** 1–18
[5] Nogueira D A, da Silveira J M, Vidal E M, Ribeiro N T and Burkert 2018 Cell disruption of Chaetoceros calcitrans by microwave and ultrasound in lipid extraction *Int. J. Chem. Eng.* Article ID 9508723
[6] Juttuporn W, Thiengkaew P, Rodklongtan A, Rodprapakorn M and Chitprasert P 2018 Ultrasound-Assisted Extraction of Antioxidant and Antibacterial Phenolic Compounds from Steam-Exploded Sugarcane Bagasse *Sugar Tech* **20** 599–608
[7] Guo P, Zheng C, Huang F, Zheng M, Deng Q and Li W 2013 Ultrasonic pretreatment for lipase-catalyzed synthesis of 4-methoxy cinnamoyl glycerol *J. Mol. Catal. B Enzym.* **93** 73–8
[8] Merouani S, Hamdaoui O, Rezgui Y and Guemini M 2013 Effects of ultrasound frequency and acoustic amplitude on the size of sonochemically active bubbles-Theoretical study *Ultrason. Sonochem.* **20** 815–9
[9] Gadhe A, Sonawane S S and Varma M N 2014 Ultrasonic pretreatment for an enhancement of biohydrogen production from complex food waste *Int. J. Hydrogen Energy* **39** 7721–9
[10] Vivek K, Subbarao K V. and Srivastava B 2016 Optimization of postharvest ultrasonic treatment of kiwifruit using RSM *Ultrason. Sonochem.* **32** 328–35
[11] Khajehesamedini A, Sadatshojaie A, Parvasi P, Reza Rahimpour M and Mehdi Naserimojarad M 2018 Experimental and theoretical study of crude oil pretreatment using low-frequency ultrasonic waves *Ultrason. Sonochem.* **48** 383–95
[12] Giacometti J, Žauhar G and Žuvić M 2018 Optimization of Ultrasonic-Assisted Extraction of Major Phenolic Compounds from Olive Leaves (Olea europaea L.) Using Response Surface Methodology *Foods* **7** 149
[13] Sajjadi B, Asaithambi P, Abdul Aziz A R and Ibrahim S 2016 Mathematical analysis of the effects of operating conditions and rheological behaviour of reaction medium on biodiesel synthesis under ultrasound irradiation *Fuel* **184** 637–47
[14] Luo J, Fang Z and Smith R L 2014 Ultrasound-enhanced conversion of biomass to biofuels *Prog. Energy Combust. Sci.* **41** 56–93
[15] Rayleigh 1917 On the pressure developed in a liquid during the collapse of a spherical cavity *London, Edinburgh, Dublin Philos. Mag. J. Sci.* **34** 94–8
[16] Plesset M S 1949 The dynamics of cavitation bubbles *J. Appl. Mech.* **16** 277–82
[17] Plesset M S 1977 Bubble Dynamics and Cavitation *Annu. Rev. Fluid Mech.* **9** 145
[18] Fourest T, Laurens J M, Deletombe E, Dupas J and Arrigoni M 2014 Analysis of bubbles dynamics created by Hydrodynamic Ram in confined geometries using the Rayleigh-Plesset equation *Int. J. Impact Eng.* **73** 66–74
[19] Fourest T, Laurens J M, Deletombe E, Dupas J and Arrigoni M 2015 Confined Rayleigh-Plesset equation for hydrodynamic ram analysis in thin-walled containers under ballistic impacts *Thin-Walled Struct.* **86** 67–72
[20] Keller, B. Joseph; Miksis M 1980 Bubble oscillations of large amplitude *J. Acoust. Soc. Am.* **68** 628
[21] Takeo K and Kunihiko T 2017 Finite Difference Discretisation of the Advection-Diffusion Equation *Computational Fluid Dynamics: Incompressible Turbulent Flows* pp 23–72
[22] Alehossein H and Qin Z 2007 Numerical analysis of Rayleigh-Plesset equation for cavitating water jets *Int. J. Numer. Methods Eng.* **72** 780–807
[23] Tian H, Yang C and Liao Z 2008 Numerical simulation of cavitation bubble dynamics based on different frame Rayleigh-Plesset equation *2008 Asia Simul. Conf. - 7th Int. Conf. Syst. Simul.*

Sci. Comput. ICSC 2008 1312–6
[24] Chakma S and Moholkar V S 2013 Numerical simulation and investigation of system parameters of sonochemical process *Chinese J. Eng.* Article ID 362682
[25] Merouani S, Hamdaoui O, Rezgui Y and Guemini M 2015 Mechanism of the sonochemical production of hydrogen *Int. J. Hydrogen Energy* **40** 4056–64
[26] Merouani S, Ferkous H, Hamdaoui O, Rezgui Y and Guemini M 2015 A method for predicting the number of active bubbles in sonochemical reactors *Ultrason. Sonochem.* **22** 51–8
[27] Merouani S, Hamdaoui O, Rezgui Y and Guemini M 2016 Computational engineering study of hydrogen production via ultrasonic cavitation in water *Int. J. Hydrogen Energy* **41** 832–44
[28] Tey W Y, Lee K M, Nor Azwadi Che S and Yutaka A 2019 Delfim-Soares explicit time marching method for modelling of ultrasonic wave in microalgae pre-treatment *IOP Conf. Ser. Earth Environ. Sci.* **268** 012106
[29] Narendranath A D 2016 Solution to the one-dimensional Rayleigh-Plesset equation by the Differential Transform method
[30] Ghahramani E, Arabnejad M H and Bensow R E 2019 A comparative study between numerical methods in simulation of cavitating bubbles *Int. J. Multiph. Flow* **111** 339–59
[31] Tey W Y, Yutaka A, Nor Azwadi Che S and Goh R Z 2017 Governing equations in computational fluid dynamics: Derivations and a recent review *Prog. Energy Environ.* **1** 1–19
[32] Burden R L and Faires J D 2011 Chapter 5: Initial Value Problems *Numerical Analysis* (Boston, USA: Cengage Learning) pp 260–356
[33] Chapra S C and Canale R P 2010 Runge-Kutta Methods *Numerical Methods for Engineers* (Singapore: McGraw Hill Higher Education) pp 707–51
[34] Merouani S, Hamdaoui O, Rezgui Y and Guemini M 2014 Energy analysis during acoustic bubble oscillations: Relationship between bubble energy and sonochemical parameters *Ultrasonics* **54** 227–32
[35] Le N T, Julcour-Lebigue C and Delmas H 2015 An executive review of sludge pretreatment by sonication *J. Environ. Sci. (China)* **37** 139–53
[36] Contamine R F, Wilhelm A M, Berlan J and Delmas H 1995 Power measurement in sonochemistry *Ultrason. - Sonochemistry* **2**